Hindawi Publishing Corporation
International Journal of Geophysics
Volume 2011, Article ID 216315, 13 pages
doi:10.1155/2011/216315

Research Article

Seismic Imaging and Seismicity Analysis in Beijing-Tianjin-Tangshan Region

Xiangwei Yu,[1] Wenbo Zhang,[1] and Yun-tai Chen[2]

[1] *Key Laboratory of Computational Geodynamics, Chinese Academy of Sciences, Beijing 100049, China*
[2] *School of Earth and Space Sciences, Peking University, Beijing 100871, China*

Correspondence should be addressed to Xiangwei Yu, yuxw@gucas.ac.cn

Received 13 December 2010; Revised 22 March 2011; Accepted 20 May 2011

Academic Editor: Yu Zhang

In this study a new tomographic method is applied to over 43,400 high-quality absolute direct P arrival times and 200,660 relative P arrival times to determine detailed 3D crustal velocity structures as well as the absolute and relative hypocenter parameters of 2809 seismic events under the Beijing-Tianjin-Tangshan region. The inferred velocity model of the upper crust correlates well with the surface geological and topographic features in the BTT region. In the North China Basin, the depression and uplift areas are imaged as slow and fast velocities, respectively. After relocation, the double-difference tomography method provides a sharp picture of the seismicity in the BTT region, which is concentrated along with the major faults. A broad low-velocity anomaly exists in Tangshan and surrounding area from 20 km down to 30 km depth. Our results suggest that the top boundary of low-velocity anomalies is at about 25.4 km depth. The event relocations inverted from double-difference tomography are clusted tightly along the Tangshan-Dacheng Fault and form three clusters on the vertical slice. The maximum focal depth after relocation is about 25 km depth in the Tangshan area.

1. Introduction

Beijing-Tianjin-Tangshan (BTT) region (114°E~120°E, 37.5°N~41.5°N) is situated in the northern part of North China. Figure 1 shows the major geological structure in the BTT region. This study region is under complex tectonic process with the Taihangshan uplift in the west, the Yanshan uplift in the northeast, and the North China Basin in the middle portion, which is a large continental basin and is characterized as an alternate uplift and depression zone [7, 8]. As shown in Figure 1, in the North China Basin and Taihangshan uplift, there are several active Cenozoic faults, such as Weixian-Yanqing Fault, Tongxian-Nanyuan Fault, Xiadian-Fengheying-Caojiawu Fault, and Tangshan-Dacheng Fault, that are oriented in NE-SW direction. There are also some active faults in NW-SE direction in the BTT region, such as Western Luanxian Fault, Laishui Fault, Ninghe Fault, and Nankou-Sanhe Fault.

The BTT region is a very active area with high seismicity. In this region, earthquakes are concentrated in four seismic zones: Zhangjiakou-Bohai seismic zone, Tangshan-Hejian-Cixian seismic zone, Sanhe-Linshou seismic zone, and Huailai-Weixian seismic zone. The Zhangjiakou-Bohai seismic zone in NW-SE direction is most active with a majority of large earthquakes in the BTT region. The other three seismic zones are parallel to each other in the NE-SW direction. Historically, strong earthquakes occurred frequently in this region. So far, more than 100 earthquakes with magnitude equal to and larger than 5.0 have occurred there since 780 BC. Thirty-four of them are with magnitudes larger than 6.0 and seven with magnitudes larger than 7.0. The great Tangshan earthquake (M_S = 7.8) in 1976 is one of the most destructive earthquakes in history, which totally destroyed Tangshan city and caused a casualty of ~240,000. Therefore, a detailed investigation of the crustal structure and seismicity of the BTT region is very important not only for the understanding of physics of continental earthquakes but also for the assessment and mitigation of seismic hazard.

A lot of studies have been performed in the past three decades to invert for the three-dimensional (3D) seismic velocity structure of the crust and upper mantle beneath this region using arrival times from local and/or teleseismic events [2, 9–15] as well as the seismicity in this region [16–24]. However, the spatial resolution and the accuracy of event

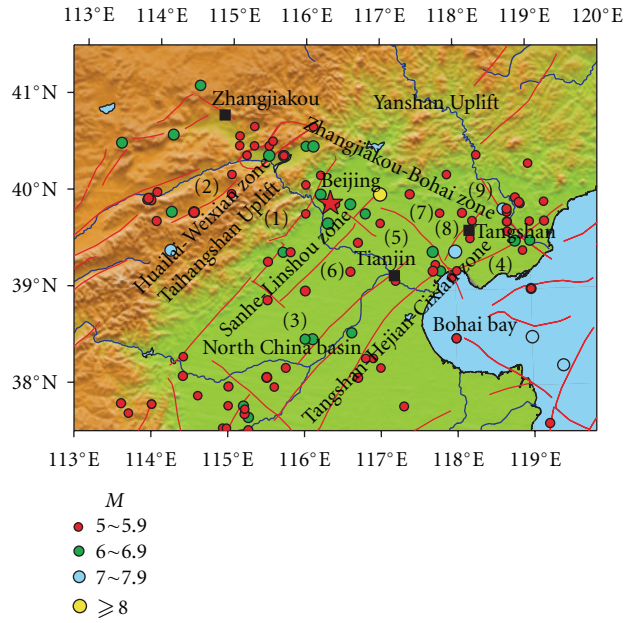

Figure 1: Geological setting and historical earthquakes in the BTT region. Colorful circles show the earthquakes with magnitudes (M) equal to or greater than 5.0 that occurred in the BTT region since 780 BC. Black squares denote major cities. Red star shows the capital of China. Thick curved lines show major active faults: (1) Tongxian-Nanyuan Fault; (2) Weixian-Yanqing Fault; (3) Laishui Fault; (4) Changli-Ninghe Fault; (5) Nankou-Sanhe Fault; (6) Xiadian-Fengheying-Caojiawu Fault; (7) Ninghe Fault; (8) Tangshan-Dacheng Fault; (9) Western Luanxian Fault.

location are limited by using only the absolute arrival times. To improve the resolution of regional tomography, some seismic tomographic techniques have been developed, such as double-difference tomography (tomoDD) [6], which uses both absolute and relative arrival time data to determine a 3D velocity structure jointly with the absolute and relative event location. Furthermore, most of the previous efforts have focused on the crustal and mantle structure [2, 9–15] whereas little effort has been devoted to the study of relationship between seismicity of small earthquakes and velocity anomaly. Where is the location of top boundary of low velocity beneath Tangshan area? What is the deepest focal depth of the relocated earthquakes inverted by tomography? What is the main dynamic source for the great Tangshan earthquake? The detailed structure of hypocentral area is still unclear beneath the Tangshan area. Determining a high-resolution 3D velocity model of the crust and upper mantle beneath this region is the key for answering these questions. The tomoDD imaging has the potential to bring substantial insight into them by using both absolute and relative arrival time data.

In this study, we apply the tomoDD method to combine absolute and relative arrival time data to invert for the detailed 3D crustal P wave velocity structure jointly with absolute and relative event locations in the BTT region. Our results will shed new light on the relationship between relocated seismicity and the 3D velocity structure.

2. Data and Method

Both absolute and relative arrival times are used in this study. We carefully select the data such that each event has at least 6 recordings (8 in the Tangshan area). The resulting data include over 43,400 high-quality absolute direct P arrival times and 200,660 relative P arrival times from 3,983 earthquakes recorded by one or more of the 112 stations of the North China Telemetry Seismic Network (NCTSN) and the Capital Digital Seismic Network (CDSN) from 1993 to 2004 in the BTT region (Figure 2). The accuracy of the first P arrival time picking is estimated to be 0.2~0.3 s. The focal depth varies from ground surface down to about 30 km depth. The ray path coverage is generally good except Bohai Bay where no seismic station is present (Figure 3).

The tomoDD, developed by Zhang and Thurber [6], is used in this study to determine a 3D velocity structure jointly with the absolute and relative event location, which is based on the hypoDD of Waldhauser and Ellsworth [5] and also uses both absolute and relative arrival time data. With standard tomography, event locations will be somewhat scattered due to imprecise picks and origin-time errors. The tomoDD method uses the differential arrival times which are free from origin-time errors, and thus it removes some fuzziness from the velocity model.

Our starting 1D model is inferred from a minimum 1D velocity model [2] for the crust (0~25 km depth) and from deep seismic soundings [25, 26] for the deeper crust and upper mantle (25~40 km depth) (Figure 4). A 3D regular grid is used in this study [27]. The velocity values are interpolated by using a trilinear interpolation method. The model has been parameterized into an optimal grid spacing of 50 km laterally and 5 km vertically after a number of resolution tests for different grid spacing. Distance weighting is used in this study to control the maximum separation between event pairs. For closer event pairs a larger weight is applied. Considering the trade-off between the roughness and the stabilization of the model, we choose the model using smoothing weight of 5 as the preferred model. Velocity structure and hypocentral parameters of the local earthquakes are all taken to be unknown parameters in the inversion. A detailed description of the method is given by Zhang and Thurber [6].

3. Seismic Tomography

Local (regional) earthquake tomography (LET) plays an important role in studying the velocity structure of the Earth's interior, which has become a relatively routine application for use in seismically active regions covered by one or more dense seismic network.

We conduct many inversions using different values of damping parameter for the variance of the velocity perturbations and root-mean-square (rms) travel time residuals. We find that the best value of the damping parameter is 150. In order to confirm the main features of our tomographic image, we conduct a resolution test to assess the adequacy of the ray coverage and to evaluate the resolution [28, 29]. An initial checkerboard velocity model is created by assigning

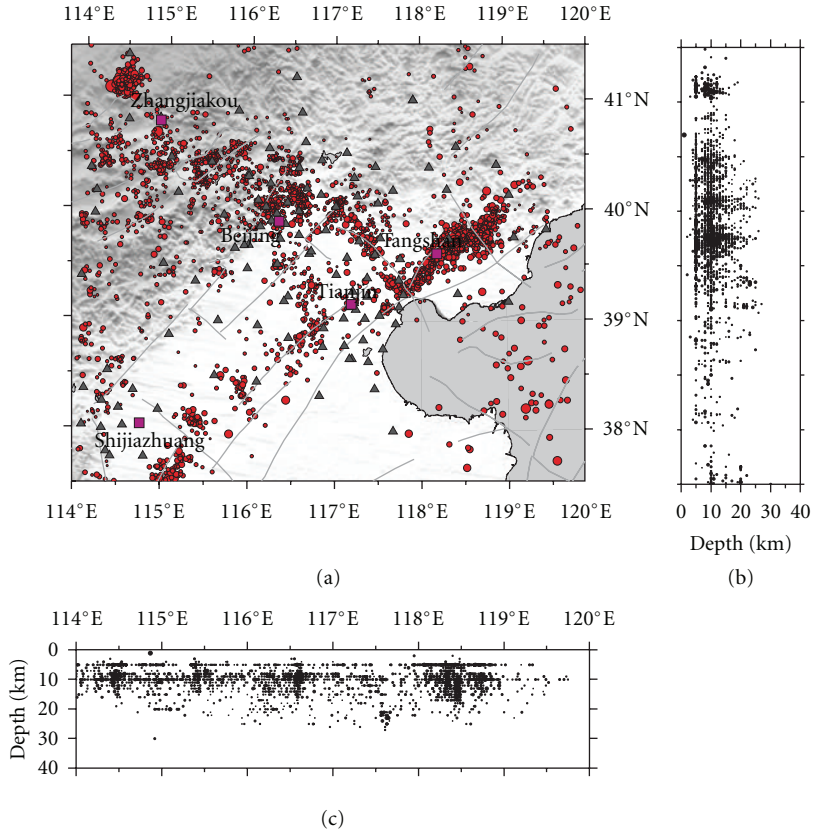

Figure 2: Distribution of seismic stations and earthquake hypocenters used in this study. (a) shows distribution of earthquake epicenters (circles) and seismic stations (triangles). Squares show the major cities. Thick lines denote active faults; (b) and (c) show the cross sectional view of focal depth along latitude and longitude profiles, respectively.

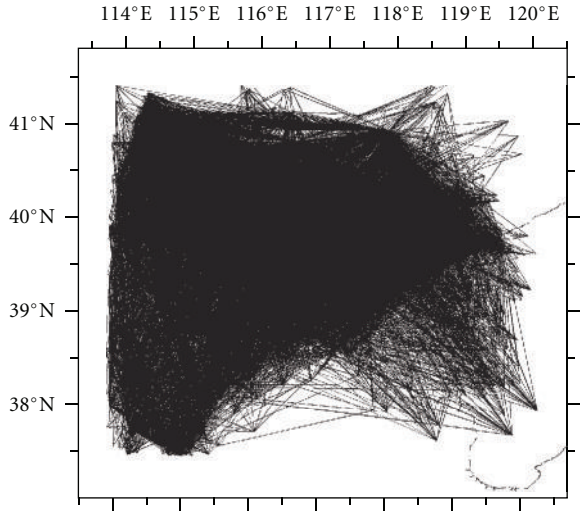

Figure 3: Distribution of P wave ray paths used in this study in map view.

alternately positive and negative velocity anomalies (3%) to the 3D grid nodes in the model space. Synthetic travel times are calculated for the checkerboard model using the real event and receiver locations. A random noise with zero mean and standard deviation of 0.1 s is added to the synthetic data. The resolution is considered to be good for regions where the checkerboard image is well recovered. Figure 5 shows the result. The checkerboard pattern is recovered for almost the entire study region except for Bohai Bay and the edge of the BTT region (Figures 5(a)–5(f)). Areas with low resolution are excluded from the resulting tomographic images (Figure 6). The best resolution is in the depth range of 5–20 km (Figures 5(a)–5(d)), where the amplitude of velocity anomalies is well recovered across the whole region. The resolution is reduced below 30 km depth. But the checkerboard positive and negative patterns are basically recovered.

In order to show more clearly the continuous variations of velocity anomalies in the depth direction, our resulting tomographic images are presented in Figure 6. In general, the results reveal strong lateral heterogeneities in both of the crust and uppermost mantle. It is noted that the media beneath the Tangshan area are very different from adjacent areas throughout the crust and upper mantle. In the shallow depth (Figures 6(a) and 6(b)), the inversion results are consistent with the local geological settings and follow the trend of active faults in the BTT region. The tomographic images illustrate that the low P velocity (low-V) anomalies exist beneath depressions and basins (such as the North China Basin) and high P velocity (high-V) anomalies exist

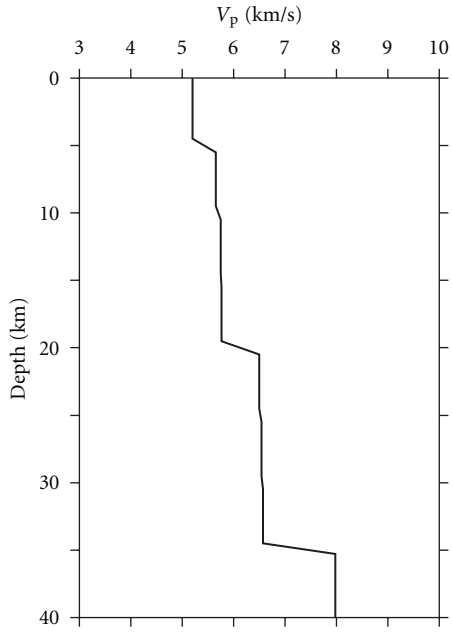

Figure 4: The starting 1D model used for the tomoDD in this study.

beneath mountains and uplifts (such as Yanshan uplift and Taihangshan uplift), which is consistent with the previous standard tomographic studies [2, 9–15]. But our model has sharper velocity contrasts near the boundary between low-V and high-V anomalies than previous tomography models do. Although the Tangshan area is located in the North China Basin, it is an uplifted block beside the Zhangjiakou-Bohai seismic zone [21]; hence, it shows up as high-V anomaly. At the 35 km depth, our present result has revealed that a broad and prominent low-V anomaly exists beneath the Taihangshan uplift area and the Tangshan area, and high-V anomaly exists beneath the Yanshan uplift and the North China Basin. These results are consistent with the P_n tomographic results [15, 30, 31].

Several cross-sections along the different longitudes (115.5°E, 116.5°E, 117.5°E, and 118.5°E) and latitudes (40.5°N, 39.8°N, and 39.0°N) are presented in Figure 7. At shallow depth (5∼10 km), the boundary between the low-V anomaly and high-V anomaly is well consistent with the boundary between mountain/uplift and plain/basin, such as the 39.5°N area at the 115.5°E profile (Figure 5(a)) and 118.0°E area at the 39.8°N profile (Figure 7(b)). Our tomoDD model shows a high-V anomaly of ∼90 km length at 10∼20 km depth under the Beijing, Tianjin, and the Tangshan area at the profile of 116.5°E, 117.5°E, and 118.5°E (Figure 5(a)). A prominent broad low-V anomaly is discovered from 20 km to 30 km both beneath Yanshan uplift, the North China Basin area at the profile of 115.5°E (Figure 5(a)), and beneath the Tangshan area at the profile of 118.5°E (Figure 5(a)). At the profile of 39.8°N (Figure 5(b)), the P velocity is high beneath the east of the Tangshan area, where there is uplift block near the Zhangjiakou-Bohai seismic zone. Moreover, it can also be found that a broad high-V anomaly beneath the Taihangshan uplift extends toward the east and down to ∼20 km depth beneath the Beijing area.

4. Relationship between Seismicity and Tomography Image in the BTT Region

An advantage of the tomoDD is that it determines the 3D velocity model as well as the absolute and relative event location compared with standard tomography. We analyzed 3,983 earthquakes with magnitudes from M 1.0 to 6.2 recorded by 112 stations. An event will be excluded from the inversion if it cannot be connected to any other events, and as a result only 2,809 hypocentral parameters of both absolute and relative locations are given by the tomoDD. The weighted rms travel-time residuals decrease from 1.2 s to 0.3 s. Figure 2 shows the catalog locations, which are scattered along major active fault zone both in horizontal direction and depth direction due to imprecise picks, origin-time errors, and simple 1D velocity model. After relocation, the tomoDD method provides a sharp picture of the seismicity in the BTT region, which is concentrated along with the major faults in a shape of alignment (Figure 8).

To illuminate the relationship between seismicity and velocity anomaly, we present our tomographic images together with hypocentral locations of both relocated earthquakes within 5 km off each layer depth and historic earthquakes ($M \geq 6.0$) that occurred in the BTT region (Figure 9). Although we do not know the accurate focal depths of the historic earthquakes, the statistic analysis of focal depth after the tomoDD relocation [32] suggests that most of earthquakes that occurred in the middle and lower crust under the BTT region and the North China are mainly clustered at 1∼24 km depth. In the tomographic image of 10 km and 15 km depth (Figure 9), both the relocated earthquakes and historic earthquakes have a similar feature, that is, most of the earthquakes are located in the conjunctional areas of low-V and high-V anomalies. They are slightly closer to the high-V anomaly areas. The epicentral location of the 1976 Tangshan earthquake, the 1976 Luanxian earthquake, and the 1679 Sanhe earthquake is in the transitional area closer to the high-V anomalies. It is notable that the distribution of relocated small earthquakes is consistent with the trend of high-V anomalies under the Beijing-Tangshan area. Maybe it suggests that the conjunctional zones of low-V and high-V anomalies represent weak sections of the seismogenic crust. The tectonic stresses are prone to being accumulated in the "brittle" high-V anomalies area, and hence the earthquake ruptures happened closer to the high-V anomalies zones. The locations of earthquakes, especially destructive earthquakes, are not random and are related closely to their deep structure of crust and upper mantle.

Figure 10(a) shows a cross-section along profile AA′ (Figure 10(c)) passing through the Tangshan-Hejian-Cixian seismic zone. A prominent high-V anomaly zone about 100 km in length is visible from 10 km down to 20 km depth along the Tangshan-Tianjin area, while a broad low-V anomaly exists in Tangshan and the north of the Tangshan area from 20 km down to 30 km, which is in agreement with the tomographic results of Huang and Zhao [15] using

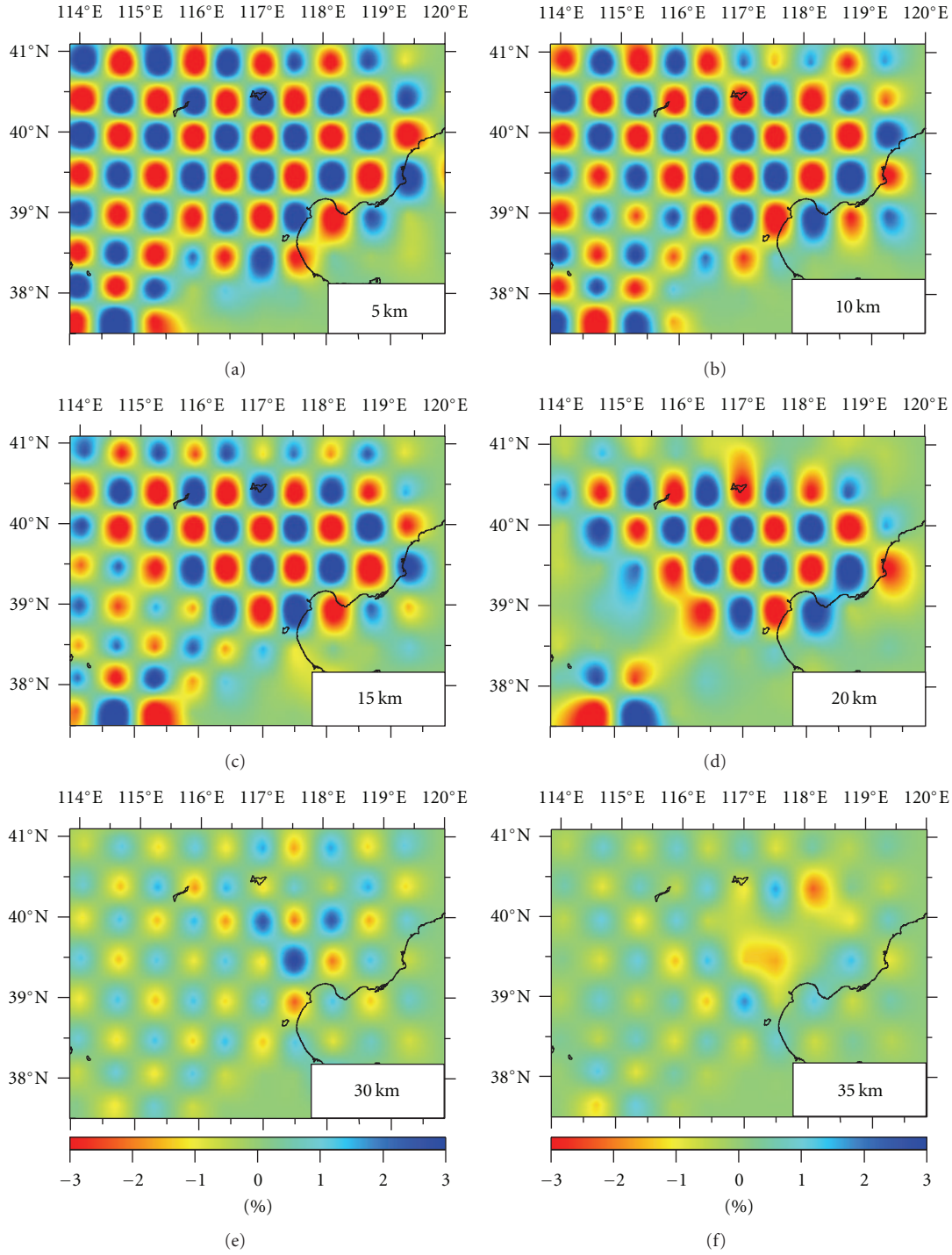

Figure 5: Results of checkerboard resolution test. The depth of the layer is shown on the right bottom of each map. The velocity perturbation scale (in %) is shown at the bottom.

local crustal earthquakes, controlled seismic explosions, and quarry blasts. Due to the differential arrival time data used to improve the precision of event location in the tomoDD, we obtained similar tomographic image only with local earthquakes. In the upper crust, the cross-sectional images show that discontinuous low-V anomalies exist under the Tangshan-Hejian-Cixian seismic zone, while, in the middle and lower crust, the low-V anomalies change to high-V anomalies. Under the Tangshan area, the maximum focal depth locates at the boundary of low-V anomaly in the middle and lower crust.

Figure 10(b) shows a cross-section along profile BB′ passing through the Zhangiakou-Bohai seismic zone. Under the Tangshan area, our result displays a transitional zone of

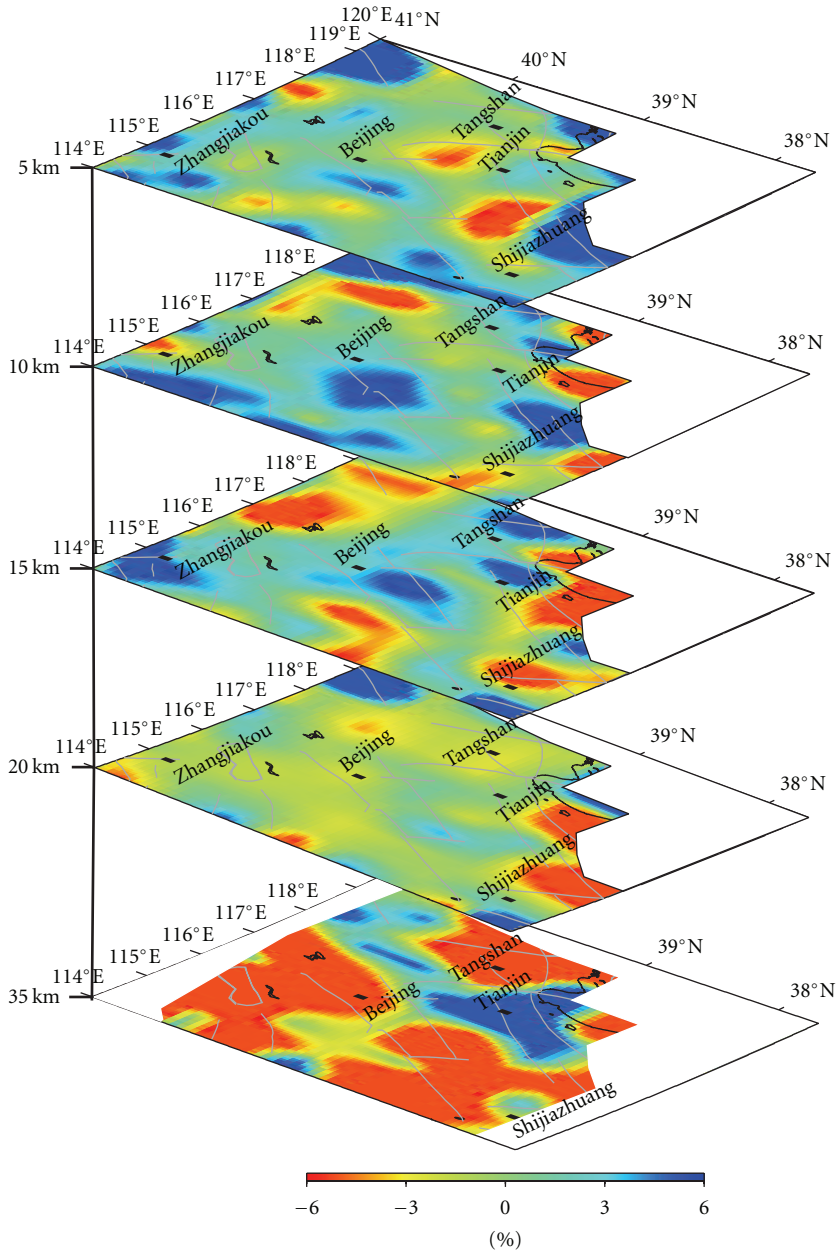

Figure 6: P wave velocity perturbation (in %) from the 1D velocity model as shown in Figure 4 at each depth slice. Red and blue colors denote slow and fast velocity anomalies, respectively. The velocity perturbation scale is shown at the bottom.

low-V anomaly in the northwest and high-V anomaly in the southeast in the upper crust, while a very prominent low-V anomaly exists in the middle and lower crust (20~30 km depth). The focal depth of relocated earthquakes that occurred in the Tangshan area is distributed in the transitional zones of low-V anomaly and high-V anomaly. In the Zhangjiakou area, the northwest of profile BB′, the deepest focal depth of relocated earthquakes with magnitude $M_L \geq 4.0$ is about 15 km, which occurred on the margin of high-V anomalies.

The Tangshan area, in the about 160 km southeast of Beijing, has the highest level of seismicity in BTT region. In this area numerous small earthquakes have occurred frequently since the great Tangshan earthquake in 1976. During 1993~2004, 118 earthquakes with $M_L \geq 3.0$ occurred in the area, 17 of them were larger than M_L4.0, such as the earthquake with M_L5.9 on 6 October 1995 and M_L5.0 on 20 January 2004 in the northeast of Tangshan.

Figure 11 shows the epicenters of earthquakes before (open circles) and after relocation (solid circles) using the tomoDD in the Tangshan area. Compared with the catalog locations, which are scattered along the fault zone, relocated hypocenters appear more clustered in the NE-SW direction along Tangshan-Dacheng fault. Figure 11 shows three clusters in different colors: the Tangshan cluster oriented in the NE-SW direction (grey solid circles), the Luanxian cluster

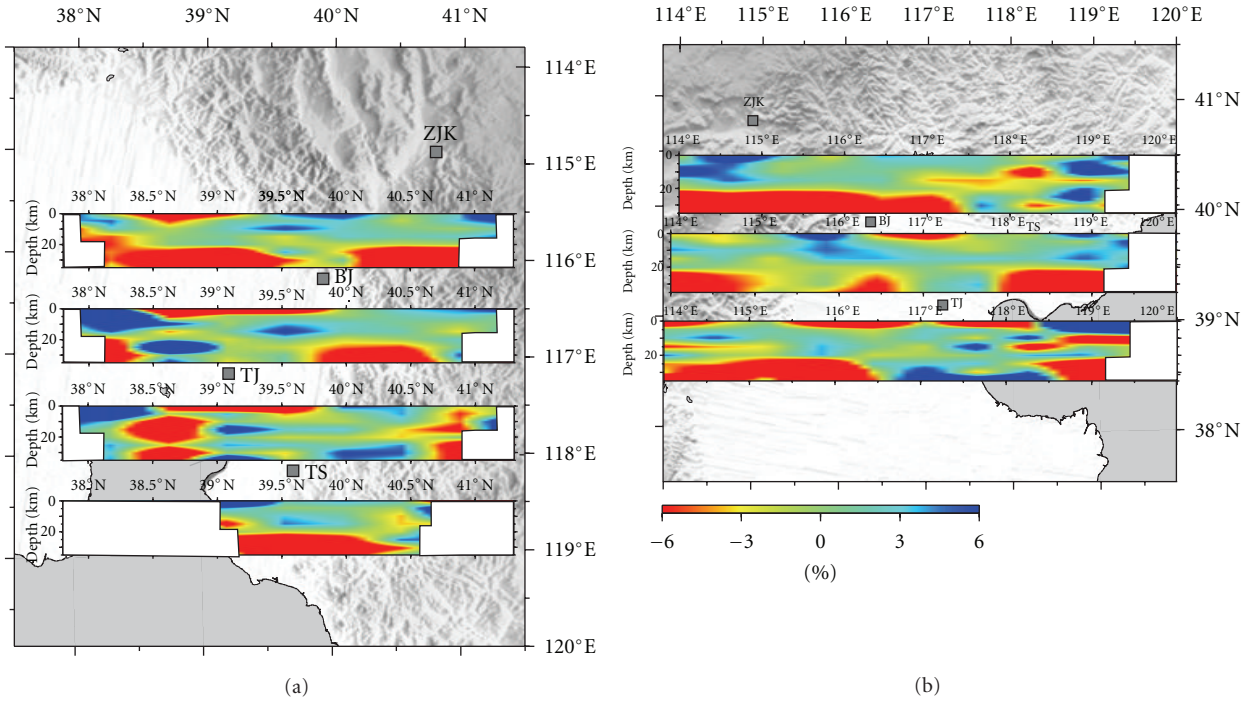

Figure 7: Vertical cross-sections of P wave velocity perturbation at each longitude (115.5°E, 116.5°E, 117.5°E, and 118.5°E) (a) and each latitude (40.5°N, 39.8°N, and 39.0°N) (b). Red and blue colors denote slow and fast-velocity anomalies, respectively. The velocity perturbation scale (in %) is shown at the bottom. BJ: Beijing; TJ: Tianjin; TS: Tangshan; ZJK: Zhangjiakou; SJZ: Shijiazhuang.

oriented nearly in the E-W direction (green solid circles), and the Qian'an cluster oriented in the NE-SW direction (blue solid circles).

In the cross-section along profile TT′ (Figure 12), the distribution of hypocenters displays a big difference between the catalog location, which is layered and scattered without clear cluster characteristic (Figure 12(a)), and the relocated location with the tomoDD, which is clustered clearly as cluster A, cluster B, and cluster C (Figure 12(b)). The Tangshan cluster (Figures 11 and 12(b), grey solid circles) becomes two clusters in depth: cluster A and cluster B. In addition, an earthquake (M_L5.9) without depth parameter before relocation is relocated in cluster A with focal depth 6.3 km.

In the cross-section along profile MN, perpendicular to TT′, the distribution of hypocenters before and after relocation using the tomoDD is also very different (Figure 13). Most of the tomoDD locations are centralized on a narrow zone within 10 km off the profile TT′ (Figure 13(b)). The earthquake relocation with $M_L \geq 4.0$ (Figure 13(b), stars) shows a near-vertical plane between 5 km and 15 km and a slight west dip between 15 km and 25 km, which is in agreement with the results of deep seismic soundings (DSSs) [33]. This indicates that the Tangshan fault is near-vertical in the shallow depth and west dip in the depth of about 22 km.

For comparison, we also relocate the events by using the DD location method, and extract the hypocenter parameters of earthquakes that occurred in the Tangshan area from previous results of the two standard tomography methods [2, 4]. The same minimum 1D velocity model [2] is used for both standard tomography and tomoDD as the initial model, which is also used for DD event location.

Figure 14 shows the event locations along profile TT′ in the Tangshan area inferred from different methods. Figure 14(a) shows the catalog locations by NCTSN. Figures 14(b) and 11(c) show the event relocations [2, 4] by the two standard tomography methods by Thurber [1] and Zhao et al. [3], respectively, where only the absolute arrival times were used for the inversion. The event locations are still scattered, similar to the catalog locations (Figure 14(a)).

Figures 14(d) and 11(e) show the event relocations by the DD location method [5] and the tomoDD method [6], respectively. In the DD location method, the weighted rms residuals decrease from 1.0 s to 0.6 s, while, in the tomoDD method, the weighted rms residuals decrease from 1.2 s to 0.3 s. After the relocation, both the DD methods provide similar features, three typical clusters under the Tangshan area. Although most of the relative event locations from the two DD methods are quite similar, there are some differences between them in detail. First, it can be noted that the absolute event locations with $M_L \geq 4.0$ are different between the two methods. The focal depth of earthquakes with $M_L \geq 4.0$ varies from 0 km to 20 km in the DD location method. In the tomoDD method, however, it varies from 5 km to 20 km. Second, in the tomoDD, earthquake relocations with $M_L \geq 4.0$ show a near-vertical plane between 5 km and 15 km and a slight west dip between 15 km and 25 km, which is in agreement with the results of deep seismic soundings

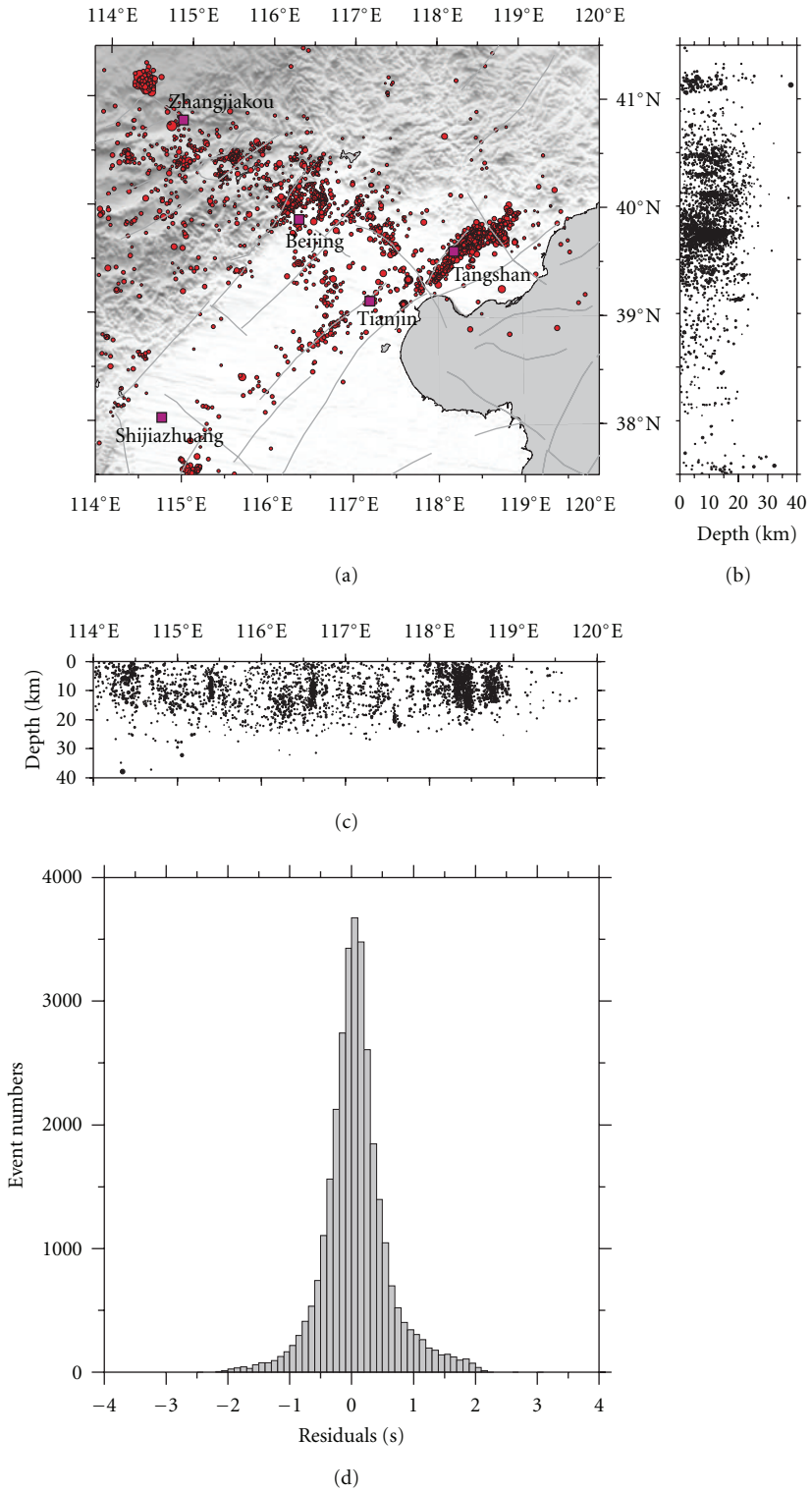

Figure 8: Earthquake hypocenters relocated in this study. (a) shows distribution of relocated earthquake epicenters (circles); squares show the major cities. Thick lines denote active faults; (b) and (c) show the cross-sectional view of focal depth along latitude and longitude profiles, respectively; (d) denotes histogram of P wave absolute travel-time residuals after relocation using tomoDD method.

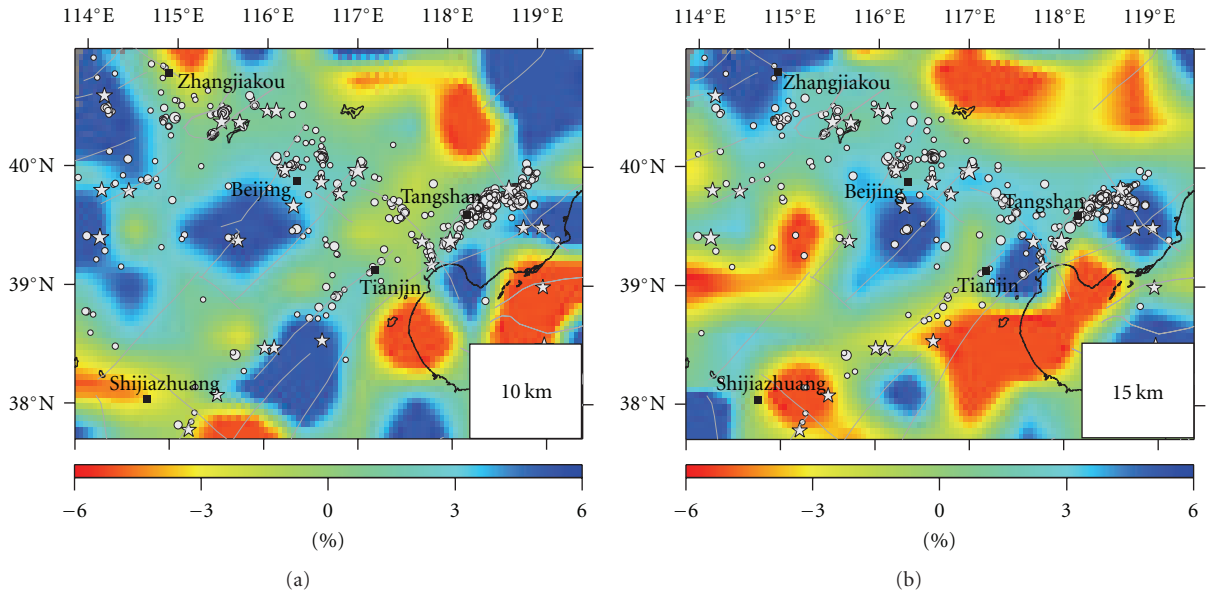

Figure 9: (a) and (b) show the map view of P wave velocity perturbations (in %) and distribution of relocated earthquake hypocenters at 10 km and 15 km, respectively. The white circles denote small earthquakes within 5 km off the different layer depth. The white stars show historic earthquake hypocenters ($M \geq 6.0$). Red and blue colors denote slow- and fast-velocity anomalies, respectively. The velocity perturbation scale (in %) is shown at the bottom.

(DSS) [33], while no such dipping is observed in the DD location method.

Figure 15 shows the velocity perturbations, resulting from the tomoDD, along the vertical cross-section of profile TT′ passing through the Tangshan area and the seismicity in this area. Only earthquakes that occurred within 0.25° off profile TT′ are chosen to project on the vertical slice. It can be clearly seen that all of the three clusters (Figure 12(b)) are relocated in the conjunctional area of low-V and high-V anomalies, slightly closer to the high-V anomaly zones. Only a few earthquakes have ever occurred within the low-V anomalies. The maximum focal depth (about 25.4 km) locates in the uppermost boundary of low-V anomaly from 20 km to 30 km under the Tangshan area. Our results suggest that the top boundary of low-V anomalies is at about 25.4 km depth in the Tangshan area, which is different from results obtained by previous standard tomography studies [15]. This indicates that the top boundary of low-V anomalies is at 20 km depth in the Tangshan area, which is consistent with the maximum of focal depth of relocation by the tomoDD.

Our tomographic results show an evident low-velocity anomaly in the lower crust beneath the BTT region (Figures 6, 7, 10(a), and 10(b)), specially beneath the Tangshan area. The results of S structure by using receiver function method [34] showed that there exist obvious heterogeneous low-V media in the upper mantle and middle crust and the crust-mantle boundary had an obvious uplift beneath the Tangshan area. Thus the existence of prominent low-V anomalies in the lower crust may suggest that there is probably massive intrusion derived from the upper mantle beneath the Tangshan area. Our tomographic results of the crust and upper mantle support such a conclusion. The main dynamic source for the Tangshan earthquake is the vertical movement of the upper mantle, which leads to material and energy exchange between the crust and upper mantle [34]. The long-term influence of the upwelling of mantle materials on the seismogenic layer would change the stress distribution and compositional evolution of fault zones, and the stresses are easier to concentrate on the high-V media, which would lead to the mechanical failure and the earthquake occurrence.

5. Conclusions

The tomoDD method is efficient in relocating a large number of earthquakes accurately and in characterizing the local velocity structure with high resolution. With this approach a high-resolution tomography model of crust and upper mantle under the BTT region has been obtained by using both absolute and relative arrival times of local earthquakes recorded by NCTSN or DCSN. Simultaneously, our results provide accurate hypocentral parameters of both absolute and relative event locations in the BTT region. The velocity images of the upper crust correlate well with the surface geological and topographic features. In the North China Basin, the depression and uplift areas are imaged as slow and fast velocities, respectively. A broad low-V anomaly exists in Tangshan and the north of the Tangshan area from 20 km down to 30 km depth, which suggests that there is probably massive intrusion derived from the upper mantle beneath the Tangshan area. Our results suggest that the top boundary of low-V anomalies is at about 25.4 km depth in the Tangshan area.

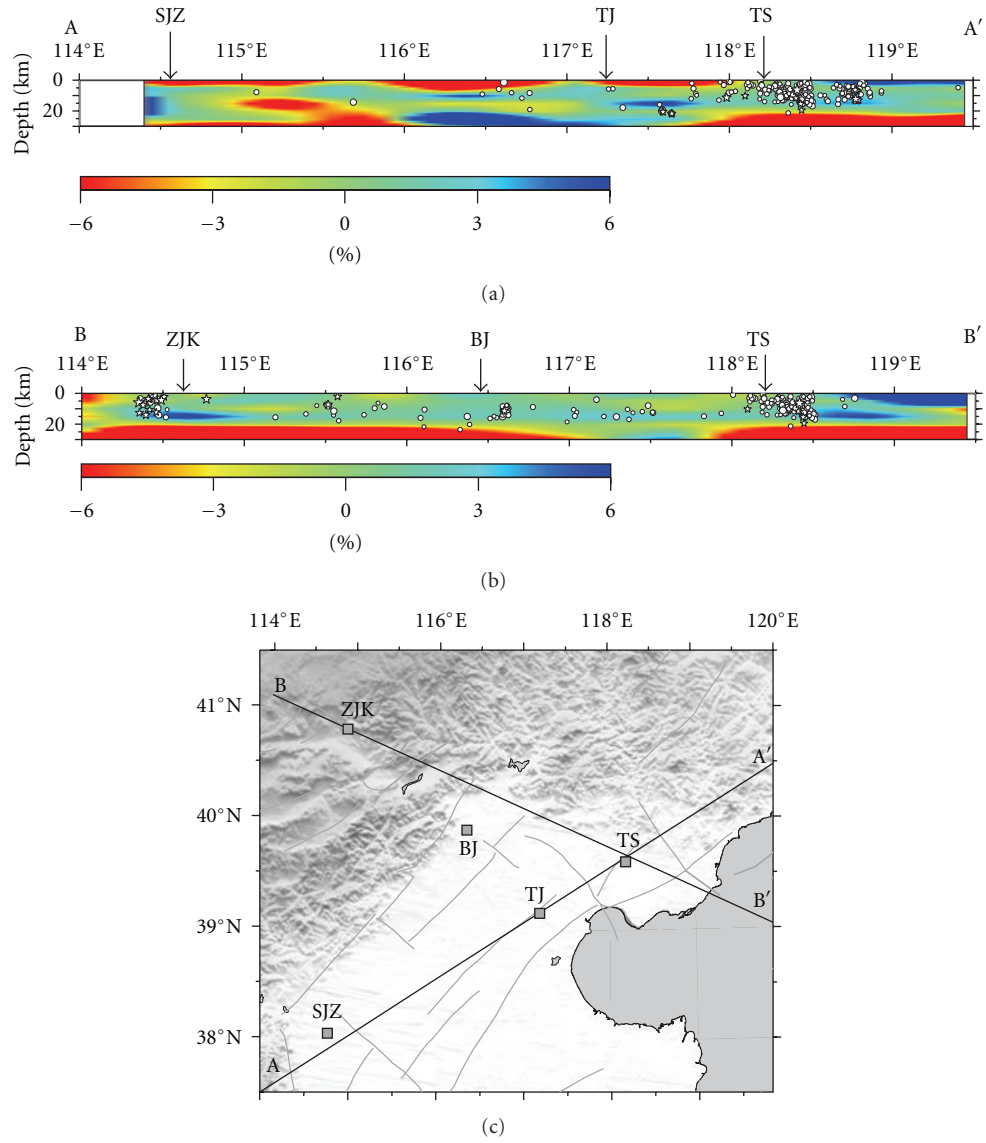

Figure 10: (a) and (b) show the vertical cross-sections of P wave tomographic image along the profiles. White stars and circles denote the earthquakes of $M_L \geq 4.0$ and $M_L < 4.0$, respectively, which occurred within 0.25° off the profile. Red and blue colors denote slow- and fast-velocity anomalies, respectively. No vertical exaggeration. (c) shows the location of profiles. BJ: Beijing; TJ: Tianjin; TS: Tangshan; ZJK: Zhangjiakou; SJZ: Shijiazhuang.

After relocation, the tomoDD method provides a sharp picture of the seismicity in the BTT region, which is concentrated along with the major faults in a shape of alignment. The seismicity of both the relocated earthquake hypocenters and the historic earthquakes shows that majority of the hypocenters are located in the conjunctional areas of low and high P wave velocity anomalies. And they are slightly closer to the high P wave velocity abnormal areas. Only a few earthquakes have epicenters in either high or low P wave velocity areas. It might suggest that the conjunctional zones of low-V and high-V anomalies represent weak sections of the seismogenic crust. The tectonic stresses are prone to being accumulated in the "brittle" high-V anomalies area and hence the earthquake ruptures happened closer to the high-V anomalies zones.

The surface event relocations in the Tangshan area are centered along the Tangshan-Dacheng fault. In the vertical slice along profile TT′, all the earthquakes are clustered in three clusters as shown in Figure 9(b), two clusters lie beneath the Tangshan-Ninghe fault, and another one lies beneath the Luanxian area. The maximum of focal depth of relocated earthquakes is 25 km, where there is the top boundary of low-V anomalies beneath the Tangshan area.

Acknowledgments

The authors thank Dr. Haijiang Zhang for providing his tomoDD code and thoughtful discussions. This work was supported by a grant from the National Natural Science Foundations of China (40404002) to X. Yu as well as a

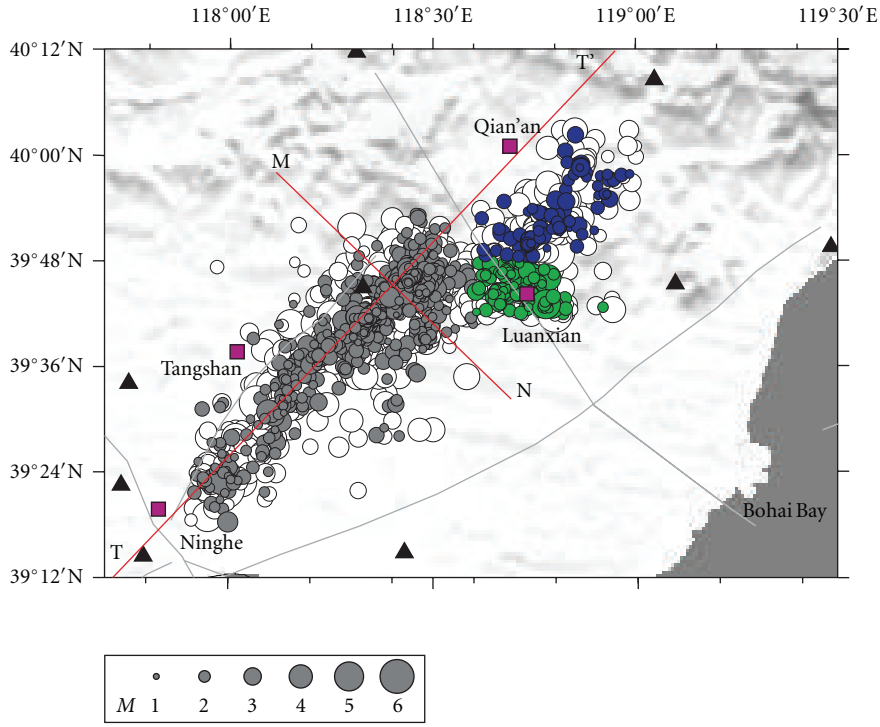

Figure 11: Epicentral distribution of earthquakes before (open circles) and after (solid circles) relocation using the tomoDD in the Tangshan area.

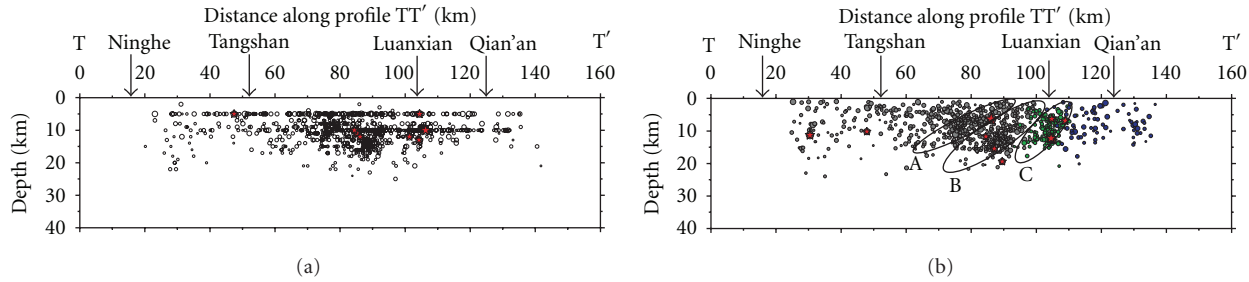

Figure 12: Cross-section along profile TT′ of focal depth before (a) and after (b) relocation using tomoDD in the Tangshan area. Stars and circles show the earthquakes of $M_L \geq 4.0$ and $M_L < 4.0$, respectively. The epicentral locations of earthquakes with different colors in Figure 12(b) are the same as in Figure 11.

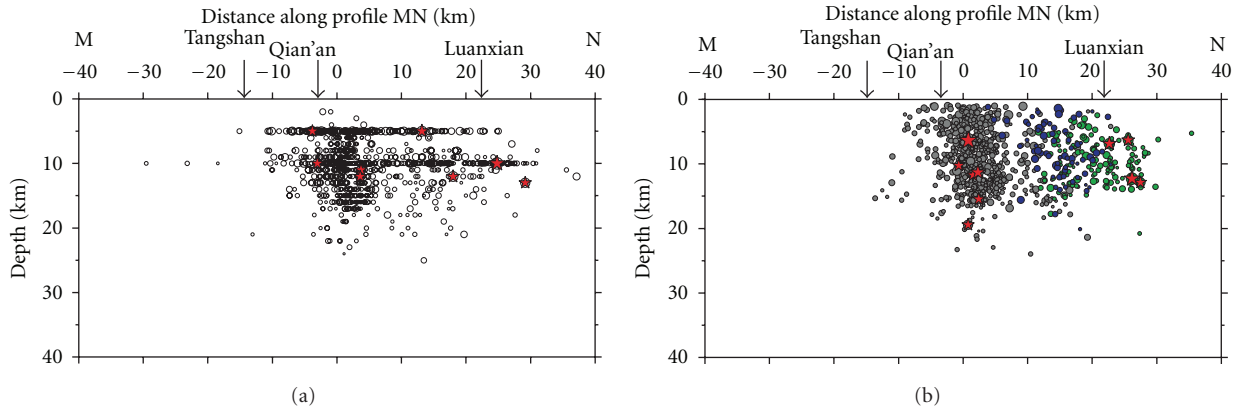

Figure 13: Cross-section along profile MN of focal depth before (a) and after (b) relocation using tomoDD in the Tangshan area. Origin of coordinates is set at the intersection point of MN and TT′. Other symbols are the same as in Figure 12.

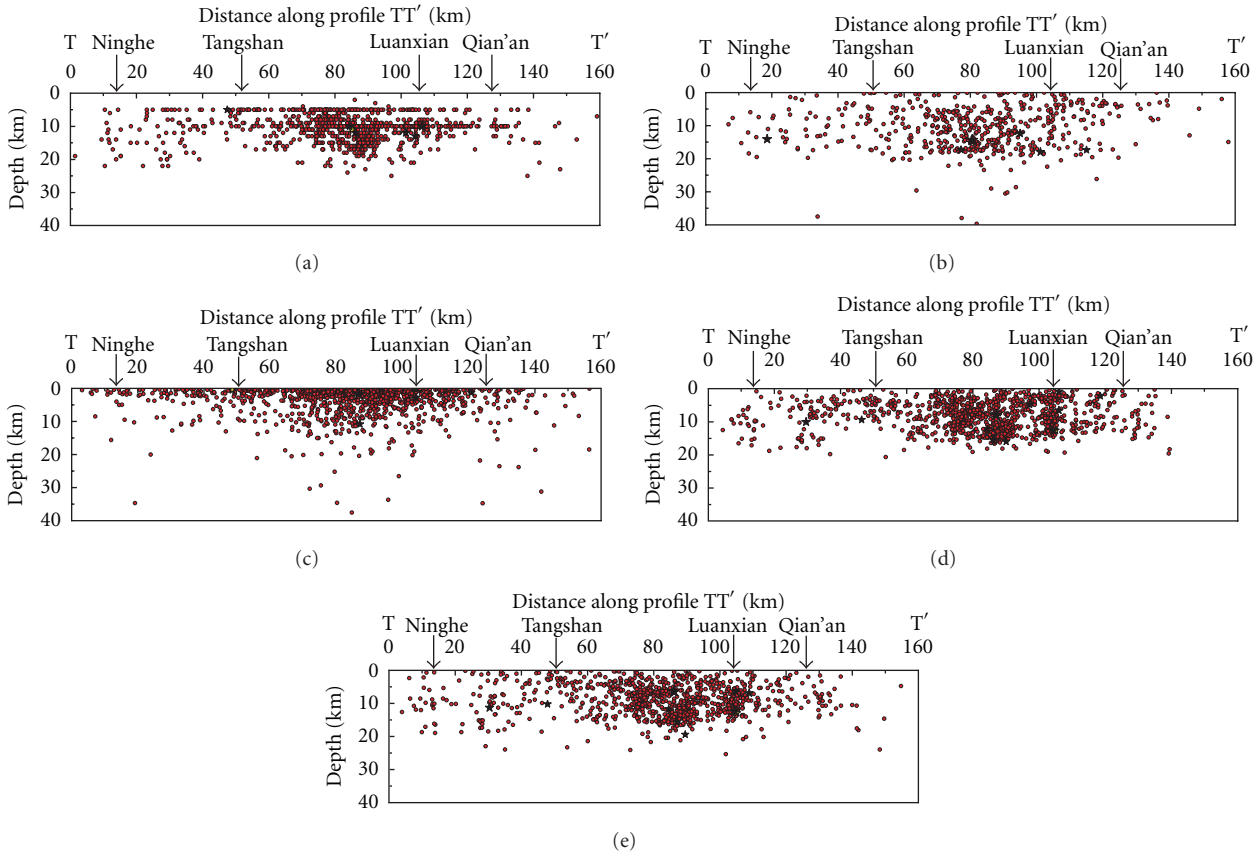

Figure 14: Cross-section of focal depth along the profile TT′ by various methods in the Tangshan area. Stars and circles show the earthquakes of $M_L \geq 4.0$ and $M_L < 4.0$, respectively. (a) Distribution of focal depth by Capital Digital Seismic Network and North China Telemetry Seismic Network; (b) distribution of focal depth using local tomography with Thurber [1] method [2]; (c) distribution of focal depth using seismic tomography with Zhao et al. [3] method [4]; (d) distribution of focal depth using DD location method [5]; (e) distribution of focal depth using tomoDD method [6].

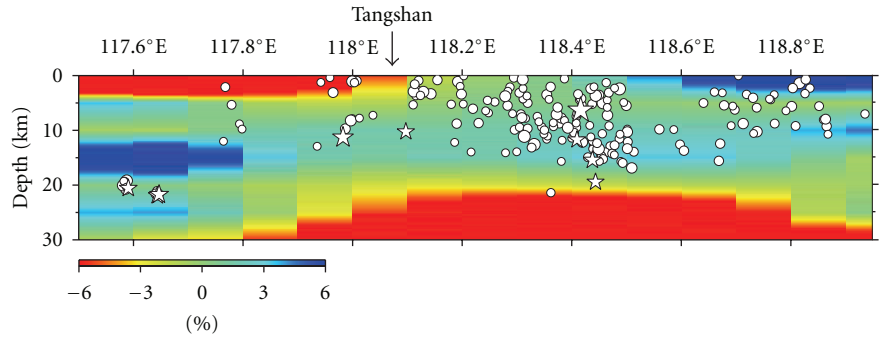

Figure 15: Vertical cross-section of P wave tomographic image along profile TT′ in Tangshan area. White stars and circles denote the earthquakes of $M_L \geq 4.0$ and $M_L < 4.0$, respectively, the occurred within 0.25° off the profile. Red and blue colors denote slow and fast velocity anomalies, respectively. No vertical exaggeration. The location of profile TT′ is shown in Figure 11.

grant from the National Natural Science Foundations of China (90715019) to W. Zhang and by the Special Research Project in Earthquake Science, CEA, to Y.-T. Chen (no. 200808068). The figures were made by using GMT [35]. They also thank the editor (Professor Y. Zhang) and four anonymous referees for their constructive comments and suggestions which improved the paper.

References

[1] C. H. Thurber, "Earthquake locations and three-dimensional crustal structure in the Coyote Lake area, central California," *Journal of Geophysical Research*, vol. 88, no. 10, pp. 8226–8236, 1983.

[2] X. Yu, Y. T. Chen, and P. D. Wang, "Three-dimensional P wave velocity structure in Beijing-Tianjin-Tangshan area," *Acta*

Seismologica Sinica, vol. 25, no. 1, pp. 1–14, 2003 (Chinese), (with English abstract).

[3] D. Zhao, A. Hasegawa, and S. Horiuchi, "Tomographic imaging of P and S wave velocity structure beneath northeastern Japan," *Journal of Geophysical Research*, vol. 97, no. 13, pp. 19909–19928, 1992.

[4] X. W. Yu, *Theory of Regional Seismic Tomography and Applications in Northern China*, Ph.D. thesis, Institute of Geophysics, CSB, Beijing, China, 2003, (in Chinese with English abstract).

[5] F. Waldhauser and W. L. Ellsworth, "A Double-difference earthquake location algorithm: method and application to the Northern Hayward fault, California," *Bulletin of the Seismological Society of America*, vol. 90, no. 6, pp. 1353–1368, 2000.

[6] H. J. Zhang and C. H. Thurber, "Double-difference tomography: the method and its application to the Hayward fault, California," *Bulletin of the Seismological Society of America*, vol. 93, no. 5, pp. 1875–1889, 2003.

[7] H. Ye, K. Sheldlock, and S. Hellinger, "The North China basin: an example of a Cenozoic rifted intraplate basin," *Tectonics*, vol. 4, no. 2, pp. 153–169, 1985.

[8] H. Ye, B. Zhang, and F. Mao, "The Cenozoic tectonic evolution of the Great North China: two types of rifting and crustal necking in the Great North China and their tectonic implications," *Tectonophysics*, vol. 133, no. 3-4, pp. 217–227, 1987.

[9] A. S. Jin, F. T. Liu, and Y. Z. Sun, "Three-dimensional P velocity structure of the crust and upper mantle under the Beijing region," *Chinese Journal of Geophysics*, vol. 23, no. 2, pp. 172–182, 1980 (Chinese), (with English abstract).

[10] F. T. Liu, K. X. Qu, and H. Wu, "Seismic tomography of North China region," *Chinese Journal of Geophysics*, vol. 29, no. 5, pp. 442–449, 1986 (Chinese), (with English abstract).

[11] K. M. Shedlock and S. W. Roceker, "Elastic wave velocity structure under the crust and upper mantle beneath the North China," *Journal of Geophysical Research*, vol. 92, pp. 9327–9350, 1987.

[12] L. P. Zhu, R. S. Zeng, and F. T. Liu, "3-D P wave velocity structure under the Beijing network area," *Chinese Journal of Geophysics*, vol. 33, no. 3, pp. 267–277, 1990 (Chinese), (with English abstract).

[13] R. M. Sun and F. T. Liu, "Crust structure and strong earthquake in Beijing, Tianjin, Tangshan area: I. P wave velocity structure," *Chinese Journal of Geophysics*, vol. 38, no. 5, pp. 599–607, 1995 (Chinese), (with English abstract).

[14] Z. F. Ding, *Regional Seismic Tomography: Theory and Applications*, Ph.D. thesis, Institute of Geophysics, CSB, Beijing, China, 1999, (in Chinese with English abstract).

[15] J. L. Huang and D. P. Zhao, "Crustal heterogeneity and seismotectonics of the region around Beijing, China," *Tectonophysics*, vol. 385, no. 1–4, pp. 159–180, 2004.

[16] Y. T. Chen, L. R. Huang, and B. H. Lin, "A dislocation model of the Tangshan earthquake of 1976 from inversion of geodetic data," *Chinese Journal of Geophysics*, vol. 22, no. 3, pp. 201–217, 1979 (Chinese), (with English abstract).

[17] R. S. Zeng, H. H. Lu, and Z. F. Ding, "Seismic refraction and reflection profilings across Tangshan epicentral region and their implication to seismogenic processes," *Chinese Journal of Geophysics*, vol. 31, no. 4, pp. 383–397, 1988 (Chinese), (with English abstract).

[18] W. X. Gao and J. Ma, Eds., *Seismo-Geological Background and Earthquake Hazard in Beijing Area*, Seismological Press, Beijing, China, 1993, (in Chinese).

[19] S. Y. Wang, Z. H. Xu, and Y. X. Yu, "Relocation of micro earthquakes in Beijing and its neighbouring areas and its tectonic implication," *Earthquake Research in China*, vol. 11, no. 3, pp. 257–269, 1994 (Chinese), (with English abstract).

[20] S. Y. Wang, Z. H. Xu, and Y. X. Yu, "Relocation of micro earthquakes in northwestern Beijing," *Acta Seismological Sinica*, vol. 7, no. 1, pp. 33–41, 1995 (Chinese), (with English abstract).

[21] C. F. Xu, "The cause of formation of the upper mantle and crust high conductive layers in Chinese mainland and the study of Tangshan earthquake," *Earth Science Frontiers*, vol. 10, supplement, pp. 102–111, 2003 (Chinese), (with English abstract).

[22] L. Bai, T. Z. Zhang, and H. Z. Zhang, "Multiplet relative location approach and wave correlation rectify and application," *Acta Seismological Sinica*, vol. 16, no. 6, pp. 606–615, 2003 (Chinese), (with English abstract).

[23] A. L. Zhu, X. W. Xu, and P. Hu, "Relocation of small earthquakes in Beijing area and its implication to seismotectonics," *Geological Review*, vol. 51, no. 3, pp. 268–274, 2005 (Chinese), (with English abstract).

[24] Z. H. Qiu, J. Ma, and G. X. Liu, "Discovery of the great fault of the Tangshan earthquake," *Seismology and Geology*, vol. 27, no. 4, pp. 669–677, 2005 (Chinese), (with English abstract).

[25] China Seismological Bureau, *Findings of Exploring the Crust and Upper Mantle Structure of China*, Seismological Press, Beijing, China, 1986, (in Chinese with English abstract).

[26] S. L. Li, X. K. Zhang, and Z. L. Song, "Three-dimensional crustal structure of the capital area obtained by a joint inversion of deep seismic sounding data from multiple profiles," *Chinese Journal of Geophysics*, vol. 44, no. 3, pp. 360–368, 2001 (Chinese), (with English abstract).

[27] J. Um and C. H. Thurber, "Fast algorithm for two-point seismic ray tracing," *Bulletin of the Seismological Society of America*, vol. 77, no. 3, pp. 972–986, 1987.

[28] E. Humphreys and R. Clayton, "Adaptation of back projection tomography to seismic travel time problems," *Journal of Geophysical Research*, vol. 93, no. 2, pp. 1073–1085, 1988.

[29] H. Inoue, Y. Fukao, and K. Tanabe, "Whole mantle P wave travel time tomography," *Physics of the Earth and Planetary Interiors*, vol. 59, no. 4, pp. 294–328, 1990.

[30] S. Y. Wang, Z. H. Xu, and S. P. Pei, "Velocity structure of the uppermost mantle beneath North China from Pn tomography and its implications," *Science in China*, vol. 46, supplement, pp. 130–140, 2003 (Chinese), (with English abstract).

[31] S. P. Pei, J. M. Zhao, Y. S. Sun et al., "Upper mantle seismic velocities and anisotropy in China determined through Pn and Sn tomography," *Journal of Geophysical Research B*, vol. 112, no. 5, Article ID B05312, 2007.

[32] X. W. Yu, H. Zhang, and Y. T. Chen, "Analysis of relocated earthquakes in North China region," *Journal of Geodesy and Geodynamics*, vol. 30, no. 2, pp. 29–33, 2010 (Chinese), (with English abstract).

[33] X. K. Zhang, Z. P. Zhu, and C. K. Zhang, "Crust and upper mantle structure of the Zhangjiakou-Bohai Sea seismic zone," *Active Fault Research*, vol. 6, no. 1, pp. 1–16, 1998 (Chinese), (with English abstract).

[34] Q. Y. Liu, J. Wang, and J. H. Chen, "Seismogenie tectonic environment of 1976 great Tangshan earthquake: results given by dense seismic array observations," *Earth Science Frontiers*, vol. 14, no. 6, pp. 205–213, 2007 (Chinese), (with English abstract).

[35] P. Wessel and W. Smith, "New version of the generic mapping tools (GMT) version 3.0 released," *EOS Transactions American Geophysical Union*, vol. 76, p. 329, 1995.